Space Shuttle Orbiter Aerodynamic Development

T.E. Surber* and D.C. Olsen†
Rockwell International, Downey, Calif.

This paper presents the design logic and optimization techniques that resulted in the Shuttle Orbiter aerodynamic configuration. Design requirements which are key configuration drivers are landing speed, payload center of gravity envelope, crossrange requirements, lateral-directional stability and control requirements, and flying qualities. Trade studies based on these requirements, subject to constraints on vehicle weight, establish wing, fuselage, and tail geometry, control surface size and geometry, and local contours and configuration details. Additional studies refine the configuration design in terms of wing aspect ratio, trailing edge sweep, twist, camber, forebody shaping, and vertical tail geometry.

Introduction

THE Space Shuttle is a spacecraft capable of launching a variety of payloads into Earth orbit, returning to Earth, and landing like an airplane. It is a complex flight vehicle comprised of three major elements: orbiter, external tank, and solid rocket booster. Operations will be performed from either the Eastern Test Range (ETR) at Kennedy Space Center, or the Western Test Range (WTR) at Vandenberg Air Force Base. Maximum payload capabilities will be 65,000 pounds for an easterly launch from ETR, and 32,000 pounds for launch into polar orbit inclinations from WTR. Nominal orbital altitude is approximately 150 n.mi. The Orbiter will be capable of retrieving payloads from such orbits and returning them to Earth. In addition, the Orbiter can function as a space laboratory for moderate duration missions, and provide accommodations and equipment for up to four payload specialists, as well as the normal crew of commander, copilot, and mission specialist. An on-orbit stay period of seven days is required, extended to 30 days during the operational phase of the program.

The purpose of this paper is to describe the approach taken in aerodynamic design of the Orbiter, and to present a summary of the aerodynamic characteristics of the selected vehicle. Because the Orbiter functions as both an aircraft and a spacecraft, its external features must be carefully configured to: 1) provide the protection and versatility required for orbital and atmospheric flight, and 2) provide aerodynamic performance and control necessary for unpowered descent and landing. The aerodynamic lines must ensure performance that is acceptable over the hypersonic/supersonic/subsonic speed range, while providing the required crossrange capability and landing velocity.

The paper identifies those Shuttle vehicle requirements which have a major influence on the Orbiter aerodynamic configuration, and presents a summary of the evolution of the Orbiter vehicle from initiation of the program to the current period. Key design trades to refine the configuration are discussed, and a summary of wind tunnel testing to develop and verify detailed aerodynamic characteristics is given. The final portion of the paper is devoted to a description of those characteristics.

Presented as Paper 74-991 at the AIAA 6th Aircraft Design, Flight Test and Operations Meeting, Los Angeles, Calif., Aug. 12-14, 1974; submitted Oct. 3, 1974; revision received Oct. 17, 1977.

Index categories: Aerodynamics; Configuration Design; Entry Vehicles and Landers.

*Supervisor, Orbiter Aerodynamics, Shuttle Aero Sciences. Associate Fellow AIAA.

†Aerodynamics Lead Engineer, Orbiter Aerodynamics, Shuttle Aero Sciences.

Shuttle Mission

The overall Shuttle mission profile is displayed in Fig. 1. The Shuttle mission consists of four main phases: 1) ignition and liftoff, 2) external tank separation, 3) Earth orbit operations, and 4) entry.

The aerodynamic design requirements for the Orbiter, for the most part, result from the analysis of the entry phase.

Entry Profile

The entry profile is displayed in Fig. 2. Deorbit is performed by retrofiring the orbital maneuver system (OMS), and the Orbiter descends to the atmospheric entry interface, 400,000 ft. During atmospheric entry, the Orbiter is guided in three phases to the 50,000-ft terminal approach interface altitude directly over the landing site (about 4,500 n.mi. downrange and up to 1,100 n.mi. crossrange). For the first phase of the entry profile, a constant angle of attack is commanded by the guidance system, while bank angle is modulated to maintain a specific pullout heating rate. During the second phase, range errors are nulled by angle-of-attack modulation. The third phase commences when the speed decreases to about 8,000 fps. At this point, bank angle variations are used to null range errors, and angle of attack is reduced linearly with speed to achieve the 10-deg angle of attack for maximum lift-to-drag ratio at about Mach 1.5.

Equilibrium subsonic gliding flight is achieved at about 40,000 ft. For the remainder of the gliding descent, angle-of-attack modulation is used for range control, while velocity control is maintained by drag modulation. The final approach and landing uses energy management of velocity and descent rate.

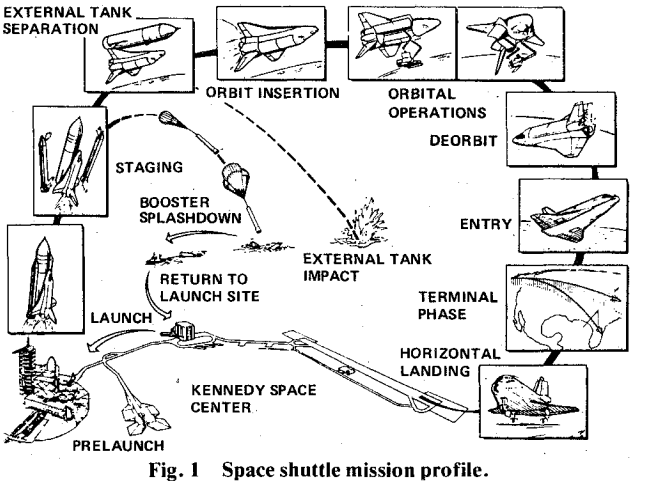

Fig. 1 Space shuttle mission profile.

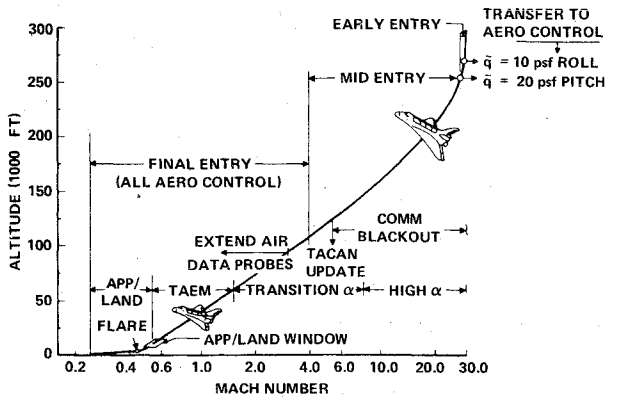

Fig. 2 Orbiter entry mission phases.

Orbiter aerodynamic requirements are established by entry mission requirements. Aerodynamic design ground rules are summarized on Table 1.

Background

Prior to initiation of the Shuttle development contract in August 1972, Rockwell International participated in extensive NASA Shuttle System contract studies. During these studies, numerous trades were conducted to determine Shuttle operational cost effectiveness, desired configuration arrangement and geometry, and major subsystem definition. In addition, the impact of mission requirement changes including payload size and weight, were also determined.

From these studies emerged a basepoint configuration at Shuttle Program authority to proceed (ATP) and a definition of the major design drivers for the Orbiter configuration. Design requirements found to be key configuration drivers are landing speed; payload size, weight, and center of gravity envelope; entry crossrange and aerodynamic heating; stability and control requirements; and flying qualities. Trade studies based on these requirements and subjected to constraints on vehicle weight established geometry and size of the wing, fuselage, vertical tail, and control surfaces, in addition to local contours and configuration details.

Table 1 Design ground rules, vehicle 5 Orbiter

Parameter	Value
Angle of attack	
Hypersonic	25 deg to 50 deg
Transonic	0 deg to 15 deg
Subsonic	−5 deg to 20 deg
Center of gravity range	
Minimum travel	2% body length
Design range	$0.65\,L_B - 0.675\,L_B$
Landing performance	
Payload	32,000 lb
Landing weight (with payload)	187,900 lb
Minimum design touchdown speed, V_D	171 knots
Longitudinal stability	
Minimum hypersonic static margin	positive
Minimum subsonic static margin (aft CG)	$-2\%\ L_B$ (−5.45% MAC)
Lift/drag modulation	
Peak subsonic value (gear-up, $\delta_{SB} = 0$ deg)	not less than 4.4
Peak subsonic value (gear-up, $\delta_{SB} = 85$ deg)	not less than 2.5

TRADE ELEMENT	ALTERNATIVES OR RANGE OF VARIABLES	BASELINE SELECTION	RATIONALE
VERTICAL TAIL DESIGN	TAIL TYPE: ℄ VERTICAL; ℄ PLUS VENTRAL; WING TIP; BUTTERFLY	℄ VERTICAL	MINIMUM WEIGHT FOR STABILITY AND HANDLING QUALITIES
	AIRFOIL: WEDGE VS. SYMMETRIC WITH 8% AND 12% THICKNESS RATIO	10° WEDGE	MINIMUM WEIGHT FOR REQUIRED STABILITY LEVEL
TAIL SCRAPE ATTITUDE	17° TO 21°	18°	REDUCED WING SIZE COMPROMISE BETWEEN REDUCED WING WEIGHT AND INCREASED GEAR WEIGHT
SPEED BRAKE LOCATION	VERTICAL TAIL VS. BODY VS. WING	VERTICAL TAIL	MULTIPLE USE WITH FLARED RUDDER; MINIMUM WEIGHT APPROACH
FOREBODY GEOMETRY	NOSE CAMBER: 0.075; 0.030	0.030	• REDUCED ELEVON SIZE TO PROVIDE DESIRED TRIM RANGE • IMPROVED INTERNAL PACKAGING AND NOSE GEAR INSTALLATION
	NOSE CROSS SECTION: A; B; C	C	• IMPROVED HYPERSONIC DIRECTIONAL STABILITY AND REDUCED SIDEWALL HEATING • ADJUSTED PLANFORM HYPERSONIC C.P. TO MEET TRIM REQUIREMENT
WING DESIGN	SWEEP 50° VS. 60° ASPECT RATIO 1.8 TO 2.4 TAPER RATIO 0.10 TO 0.30 THICKNESS 8% TO 12% TWIST 0 AND -5° AIRFOIL SYMMETRIC VS. CAMBER	50° 2.19 0.21 8% -5° CAMBER	• IMPROVED MAX C_L • IMPROVED LOW-SPEED/HIGH-SPEED AERODYNAMIC BALANCE • IMPROVED LOW-SPEED LIFT • MINIMIZED TRIM LOSSES AT LANDING • REDUCED WING SIZE
WING-BODY INTEGRATION	C.G. RANGE (% BODY LENGTH) 5% VS. 3% MAX ENTRY TRIM α (FWD C.G.) 50° VS. 35° STATIC MARGIN (AFT C.G.) -1% TO 3% DIHEDRAL 7° TO 0°	3% 50° 0% 3-1/2°	• GOOD ALLOWABLE PAYLOAD ENVELOPE WITHOUT MAJOR CONFIGURATION IMPACT • MET CROSSRANGE REQUIREMENT AND ALLOWED HIGH α ENTRY • ADEQUATE HANDLING QUALITIES REDUCED WEIGHT • IMPROVED HANDLING QUALITIES

Fig. 3 Summary of aerodynamic trade studies.

CONFIGURATION NUMBER	ATP	1 (PRR)	2A (PDR)	5 (CDR)
WING PLANFORM	50° BLENDED DELTA	50° BLENDED DELTA	45°/79° DBL DELTA	45°/81° DBL DELTA
PROFILE		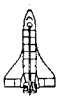		
DRY WEIGHT (LB)	170,000	170,000	150,000	150,000
PAYLOAD LBS.	40K	40K	25K	32K
C.G. RANGE % L_B	65-68%	65-68	65-67.5	65-67.5
WING AREA (FT^2)	3220.0	3220.0	2690.0	2690.0
WING SPAN (FT)	84.0	84.0	78.1	78.1
OVERALL LENGTH (FT)	124.0	125.0	125.0	122.3

Fig. 4 Orbiter evolution summary.

The ATP Orbiter basepoint configuration evolved from analyses supported by 4300 hours of wind tunnel testing. Rationale for selection of the Orbiter aerodynamic arrangement is summarized in Fig. 3. The resulting Orbiter vehicle was a blended delta wing configuration with an overall length of 124 ft and a wingspan of 80 ft. The wing was swept back 50 deg and blended into the forward fuselage to minimize wing-body interference heating. Wing size was defined by the minimum design touchdown velocity requirement. Fuselage dimensions were primarily determined by the size required to accommodate the 15×60-ft payload bay, main propulsion system, and equipment installation. The fuselage nose shape was selected by aerodynamic considerations to provide Orbiter vehicle trim and stability over the entry and subsonic flight regimes.

Upon initiation of Shuttle Program go-ahead, further trade studies were conducted to refine the basepoint design. These studies involved consideration of double-delta wing-body and canard plus delta-wing-body configuration concepts. Early in the program, changes in mission and system requirements were incorporated, resulting in a reduced size Orbiter as compared to the ATP configuration. A summary of the Orbiter evolution is presented in Fig. 4.

As a result of NASA configuration direction, the Orbiter vehicle double-delta wing configuration was selected as the best arrangement to meet requirements of the Space Shuttle mission. In selecting the basepoint design, three basic con-

figurations were evaluated: 1) blended delta wing-body, 2) double-delta wing-body, 3) canard plus delta wing-body.

The selected Orbiter resembles a contemporary delta wing aircraft. It houses the crew and payload and returns from orbit to land in a manner similar to that of a high-performance aircraft. Three large (450,000-lb thrust) liquid oxygen/liquid hydrogen rocket engines (Space Shuttle Main Engines, SSME) mounted in the aft region of the Orbiter provide propulsive thrust during ascent in addition to that provided by the Solid Rocket Boosters (SRB). Smaller rocket engines (OMS) are also located in the aft region to provide final impulse for Orbiter insertion, orbital transfer or manuevers, and deorbit. Small rocket motors referred to as the Reaction Control System (RCS) are located in both the forward and aft region for attitude control and stabilization while in orbit. The aft RCS motors are used in combination with aerodynamic surfaces for control during entry. Aerodynamic surface controls include split elevons along the wing trailing edge, a split rudder in the vertical fin which can also be flared open to serve as a speed brake during descent, and a hinged body flap located at the lower aft end of the fuselage to augment control during descent and landing approach. The body flap also shields the exposed SSME nozzles from aerodynamic heating during entry. The entire external surface of the Orbiter, except the windows, is protected by reusable insulation to maintain acceptable structural temperatures under entry heating environment.

Subsequent sections of this paper describe the effort to finalize the Orbiter aerodynamic arrangement, and to support structure and subsystem design.

Aerodynamic Design Approach

The approach to aerodynamic development of the Shuttle Orbiter is illustrated in Fig. 5. Design phases include requirements and configuration definition, configuration refinement, detail design, and design verification. The development process originated with the baseline concept at ATP, which was followed by design trade analyses and periodic updates through a series of scheduled design decisions and review. Four major reviews have been held. They are: 1) Program Requirements Review (PRR), completed November 1972; 2) System Requirements Review (SRR), completed August 1973; 3) Preliminary Design Review (PDR), completed February 1975; 4) Critical Design Review (CDR), completed August 1977.

Development of the Orbiter aerodynamic configuration is highly dependent upon wind tunnel data to support definition of aerodynamic design requirements and trade studies to finalize the configuration and to establish a continuously maturing data base for use in subsystem design and flight simulations. Approximately 10,000 wind tunnel hours were run from ATP to Orbiter PDR to finalize the configuration. Approximately 10,000 more hours are planned in support of the Orbiter aerodynamic verification and flight certification analysis.

Orbiter Aerodynamic Configuration Requirements

The approach to define the Orbiter aerodynamic configuration is illustrated in Fig. 5. Critical aerodynamic requirements were established by mission, stability and control requirements utilizing the available data and the ATP vehicle configuration as a baseline.

Development of the PRR Configuration

The aerodynamic requirements are developed primarily from analysis of the entry and landing profile displayed in Figs. 1 and 2. The requirements can be summarized as: 1) provide satisfactory controllability throughout the entire flight regime, 2) minimize aeroheating, 3) provide adequate hypersonic L/D for crossrange, 4) provide trim lift to meet landing performance requirements.

Trade studies were initiated to satisfy design requirements. The fuselage dimensions are fixed by payload size and packaging efficiency; therefore, early studies focused on development of a minimum-weight wing based on mission and payload ground rules. Landing speed is one of the key configuration drivers because of the requirement to achieve the required landing speed with a minimum-weight wing. The minimum-weight wing "system" defined for a fixed fuselage

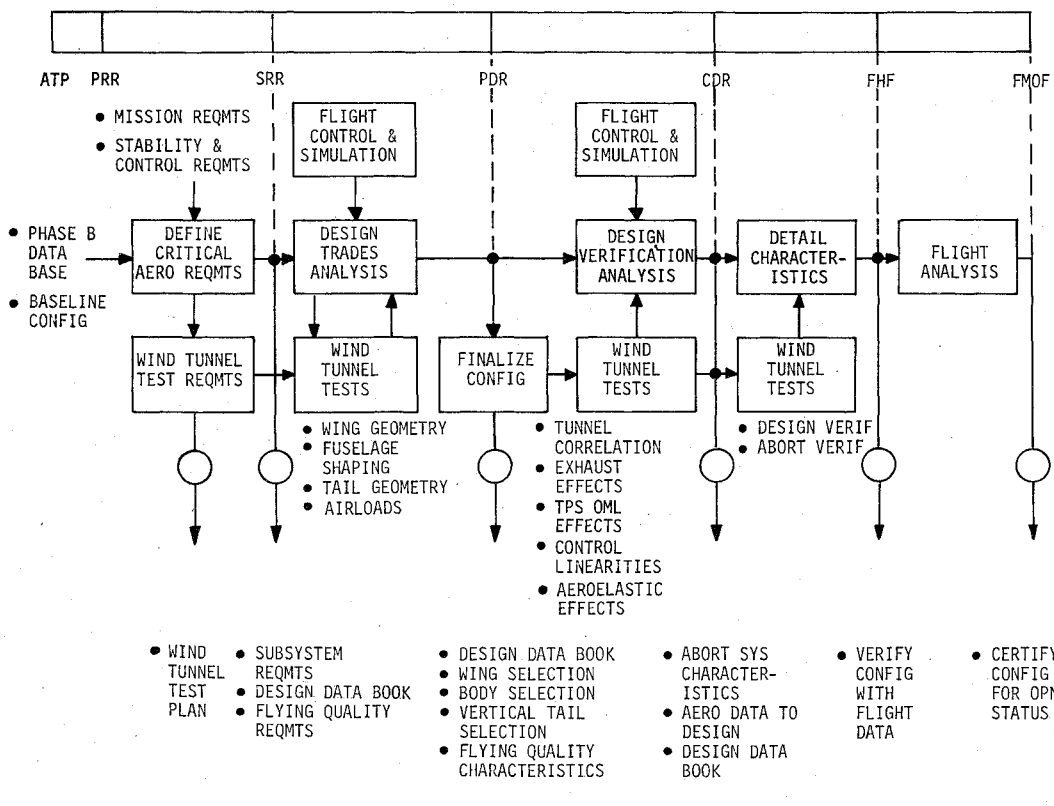

Fig. 5 Approach to definition of Orbiter aerodynamic configuration.

will thereby be the optimum wing for that particular wing-fuselage combination.

The following paragraphs of this section describe the trades (aerodynamic, thermodynamic, structures, and weights) performed to develop a minimum-weight wing based on payload and mission requirements established at ATP.

Wing Sizing

The wing "system" consists of the aerodynamic surface of the Orbiter vehicle wing-body combination. This wing-body configuration must, among other things, provide the required amount of aerodynamic lift during entry and landing, while contributing a minimum-weight fraction to the total vehicle weight. The major weight elements in this aerodynamic lifting system are the structural weight of the wing surfaces, the weight of the thermal protection system (TPS) material to protect these surfaces, and a TPS weight increment associated with the body to which the wing is attached.

To initiate the wing geometry trade study, a family of wing planform shapes was specified by selecting a series of values for the independent variables: leading edge sweep (40 deg to 60 deg), aspect ratio (2 to 4), taper ratio (0.1 to 0.3), and thickness ratio (0.04 to 0.10). The nominal center of gravity location was assumed to be at 0.66 of the body length. The landing weight of the vehicle was fixed at 170,000 lb, although a few additional calculations were made for a lighter weight of 140,000 lb.

The wing sizes defined for the trade study are based on the requirement of providing equivalent subsonic aerodynamic performance for each planform shape. The wing size is determined by landing requirements, since the wing surface provides almost all of the aerodynamic lift of the wing-body combination at subsonic speeds. The subsonic lift of the body is small compared to the wing lift, so that small changes in the body lift should have little effect on the process of wing selection and sizing. In contrast, the lower surface of the body does provide a significant amount of lift at hypersonic velocities. The hypersonic wing lift is primarily a function of exposed wing area, and is not appreciably affected by other wing geometrical parameters. The most important wing parameter affecting hypersonic performance is the leading edge sweep, which largely determines the maximum hypersonic L/D. However, adequate hypersonic L/D was achieved for the range of leading-edge sweep considered. These basic hypersonic characteristics of the wing-body make it feasible to size the wing strictly on the basis of subsonic requirements.

The initial landing requirement that defined the wing size is a design touchdown speed of 150 knots at sea level elevation on a standard day. A further constraint arose from the FAR Part 25 specification that requires this landing speed to occur at a velocity not less than 1.10 V_{stall}. The general characteristics of swept wings cause the corresponding touchdown angle of attack to increase with increasing leading-edge sweep. In order to maintain reasonable proportions for the landing gear geometry, the maximum allowable landing angle was arbitrarily limited to 17 deg. As a result, configurations with high leading-edge sweep land at a lift coefficient that is less than the fully attainable value that could be achieved by using the 1.10 V_{stall} criterion.

The aerodynamic center of the fuselage nose was found using the method of Ref. 1 with some empirical modifications to account for Orbiter nose geometry. The wing-body-nose aerodynamic center location was taken to be the weighted average of the individual aerodynamic centers with the lift coefficients being the weighting factors. In order to simplify the calculations necessary in conducting the trade study, it was decided to calculate the hypersonic center of pressure at only one angle of attack. From an inspection of previous results, it was observed that for an angle-of-attack range of from 20 to 40 deg, the center of pressure location for $\alpha = 35$ deg and zero-elevon deflection fell very near the middle of the center of gravity range, and so the center of pressure at an angle of attack of 35 deg and zero-elevon deflection was taken to represent the desired nominal center of gravity for hypersonic trim capability. The hypersonic fuselage center of pressure was determined from a Newtonian flow simulation and was located at 49.8% of the fuselage length at an angle of attack of 35 deg.

The wing center of pressure location was obtained from a comparison of hypersonic wind tunnel data and Newtonian flow predictions. For an angle of attack of 35 deg and zero-elevon deflection, the semiempirical center of pressure location was then referenced to the exposed root chord of the wing in order to facilitate the computation of the wing-body center of pressure. The wing-alone normal force coefficient was developed from a Newtonian flow model. The total hypersonic wing-body center of pressure at an angle of attack of 35 deg and zero-elevon deflection was taken to be the weighted average of the wing-alone and body-alone centers of pressure.

In order for the vehicle to be stable and trimmable for both hypersonic and subsonic velocities, it is necessary that the wing be located such that for the required center of gravity range the elevons can provide enough center of pressure control to meet the upper and lower attitude requirements at both the fore and aft centers of gravity. With the wing in this location, it was also required that the subsonic aerodynamic center be aft of the aftmost center of gravity to provide longitudinal stability.

Since for structural reasons the wing torque box must be forward of the main rocket engines, the wing may not be moved aft indefinitely. To limit this aft movement, an arbitrary limit of 50 in. was placed on the wing overhang of the fuselage (measured from the trailing edge of the exposed root chord), and any wing which needed to exceed this limit to meet the hypersonic center of pressure/center of gravity restriction was deemed unacceptable.

Too much forward wing movement is also undesirable in that it reduces the elevon's moment arm and requires a large elevon to provide the same elevon volume. Thus, another arbitrary limit of 150 in. was placed on the wing's forward movement (measured from the end of the fuselage to the trailing edge of the exposed root chord).

In this trade study, the trailing-edge sweep was unrestricted and could take on any value required to be compatible with the other wing geometry parameters. However, the sweep of the elevons is directly related to the sweep of the wing trailing edge, and too much elevon sweep will incorporate undesirable roll-yaw coupling into the vehicle's handling characteristics. Therefore, the trailing-edge sweeps of the wings were arbitrarily constrained to lie between ±20 deg and any wing whose trailing-edge sweep exceeded this range was deemed unacceptable.

Because of the large number of wing planform geometries involved, heat transfer rates for the wing were evaluated parametrically for a range of chord lengths from 10 to 60 ft. Wing section thickness ratios of 0.04, 0.06, 0.08, and 0.10 were considered. Thus, the resultant sectional heat transfer

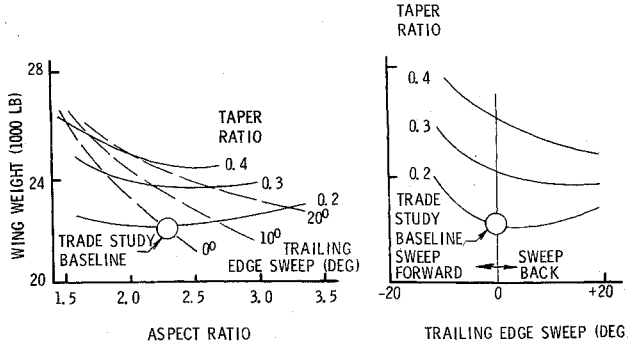

Fig. 6 Wing planform selection.

data could be applied to various combinations of wing leading-edge sweep, taper ratio, and thickness ratio by determining the appropriate chord length for a given spanwise station on the wing. Turbulent heating influences the peak heating near the wing trailing edge. The wing upper surface peak heating is governed only by laminar heating considerations.

The analysis of leading-edge maximum temperature consisted of two parts. For the first part, the maximum leading-edge temperatures were evaluated as a function of W/C_LS, leading-edge radius, and sweep angle. Maximum limits of 3460°R (100 flights without refurbishment) and 4460°R (maximum material operational limit) were applied to the temperature variations to establish ranges of useful leading-edge radii.

The results showed that the maximum temperature increased slightly with W/C_LS, but were more strongly dependent on leading-edge radius. The temperature limit lines indicated that the leading-edge radius must be approximately 1 ft to keep the maximum temperature below 3460°R, and 0.1 ft to keep the maximum temperature below 4460°R. During the second part of the study, the leading edge temperatures were evaluated for the specific wing planform geometries and airfoil sections considered in the aerodynamic analysis.

The Orbiter entry TPS selected for the wing trade study consisted of a reusable surface insulation (RSI) which covered the vehicle in areas whose surface temperatures do not exceed 2300°F. For regions such as leading edges which are above 2300°F, a reinforced carbon carbon (RCC) material was employed assumed to give 100-flight service up to 3000°F with periodic refurbishment required up to 4000°F where replacement after every mission would be necessary. The Orbiter primary structure to which the TPS is attached is made of aluminum and is designed for a maximum temperature of 350°F.

The wing structural weight was evaluated by utilizing a weight analysis computer program to calculate the weight of each candidate wing in the wing matrix. The weight analysis program calculates the torque box material dimensions required to support the shear and bending loads acting on the wing. The structure is assumed to be designed for a limit load factor of 3.0, with an additional safety factor of 1.5.

The weight of the TPS was evaluated for the wing and body surfaces. The vehicle structure is protected to a maximum temperature of 350°F by RSI system. The net effect of entry W/C_LS versus TPS weight studies was to cause a decrease in total TPS weight as the wing is made larger.

Configuration Selection, Minimum Weight System

The total wing system weight is composed of the wing structural weight, the wing TPS weight, and the incremental change in body TPS weight due to the change in entry W/C_LS.

The entry heating environment varies with exposed wing area due to the change in W/C_LS and, as a result, the TPS weight is related to the wing size. The larger wings provide a sizable reduction in the TPS material required to protect the body surfaces. Even when combined with the increased area of TPS material on the wing surfaces, the net effect is to reduce the total TPS weight for an increase in the wing size.

Effects of Planform Shape

The variation of total wing weight with planform geometry is presented in Fig. 6. The general trend that these results show is the predominant driving effect of aspect ratio on total wing weight. The effect of aspect ratio is as significant as the effect of leading-edge sweep (see also Fig. 7). An evaluation of the unit structural weight of the exposed wing panels indicated that these trends were due to the effect of aspect ratio on structural weight. The variations in total wing weight due to changes in wing area are relatively small in comparison. In addition, the expected saving in wing weight for a smaller area wing is partially compensated for by the increase in body TPS weight due to the higher entry W/C_LS associated with the smaller wing. As a result, there is no distinct advantage in incorporating the smallest, most efficient subsonic wing into the vehicle design; even if problems such as trimming such a configuration or providing thermal protection for the leading edges could be neglected.

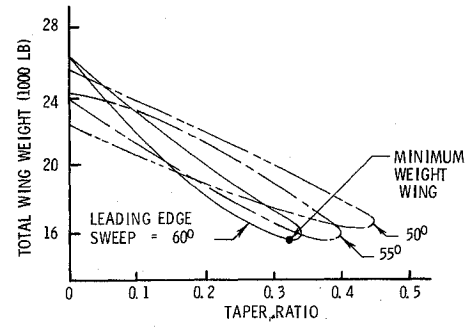

Fig. 7 Selection of minimum-weight wings.

Figure 7 illustrates the relationship between allowable wing geometry and wing weight. The illustration shows the region of acceptable wing geometry defined by the trailing-edge sweep and wing overhang constraints evaluated for a range of taper ratios. The wing weight minimizes for a leading-edge sweep of 60 deg, but only a slight weight penalty is incurred for wings with leading-edge sweep as low as 50 deg.

Additional factors considered in the wing evaluation process were the higher touchdown angle of attack and increased weight of the longer landing gear associated with higher swept wings. Consideration of these factors resulted in selection of a 50-deg leading edge, blended delta wing as the baseline for the PRR orbiter. Programmatic cost and weight decisions initiated trade studies to evaluate the effect of powered versus nonpowered landings. Based on the results of these studies, the airbreathing engine was deleted from the PRR Orbiter for orbital flight.

Trade Studies to Refine Baseline

Trade studies using the PRR Orbiter with the minimum-weight wing described in the previous section as a baseline were initiated to decrease Orbiter dry weight to 150,000 lb (PDR configuration, Fig. 4). Major changes in design ground rules to effect light weight were a decrease in hypersonic angle of attack to 40 deg, minimum subsonic static margin from zero to −2% body length (aft center of gravity), a down payload of 25,000 lb, landing weight with payload of 179,800 lb, and design touchdown speed V_D of 165 knots based on an angle of attack of 15 deg.

The wing was sized to provide a 165-knot touchdown speed (V_D) at an angle of attack of 15 deg. Detailed wing leading-edge heating studies were conducted and a 45-deg sweep was selected to provide an optimum wing leading-edge TPS with a reuse cycle of 100 flights before major rework. Forebody camber, cross section, and upward sloping sides were selected to improve hypersonic pitch trim and directional stability, and in combination with wing-body blending, to reduce entry heating on the fuselage sides. Attitude control propulsion system (ACPS) pods were incorporated with the orbital maneuvering system (OMS) and located in aft body fairings. The manipulator arm was stowed in a housing on top of the fuselage. A drogue chute was located at the base of the vertical tail and employed for braking assist to reduce rollout. A docking hatch and airlock were also incorporated into initial designs. The vertical tail was sized to provide a low-speed $C_{n_\beta} = 0.0010$ per deg at an angle of attack of 13 deg about the aft center of gravity position. The rudder was split along the Orbiter buttock plane to provide directional stability augmentation in the hypersonic/supersonic flight regimes and

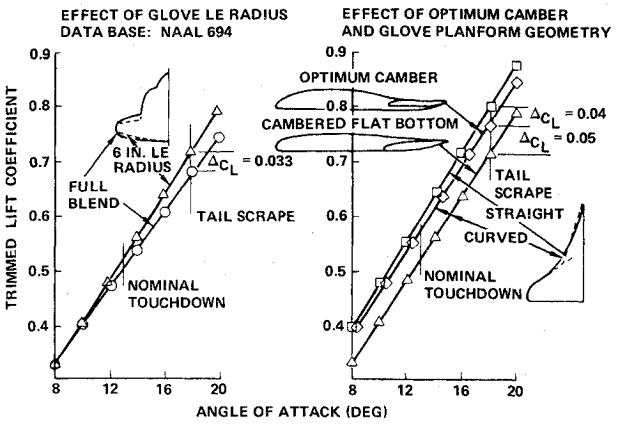

Fig. 8 Effect of configuration refinements.

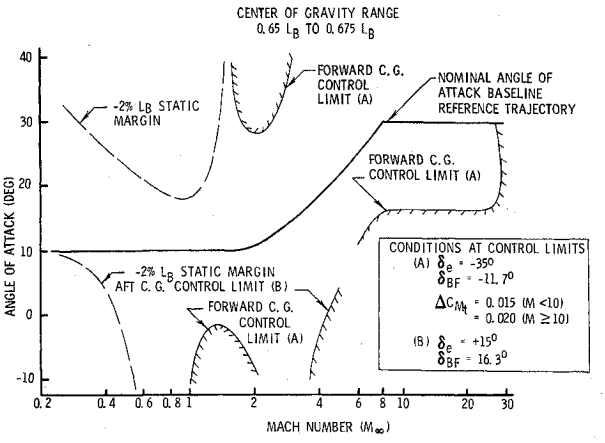

Fig. 10 Trim and stability boundaries.

GEOMETRY	WING	VERTICAL STAB.
AREA	2690 FT^2	413.25 FT^2
ASPECT RATIO	2.265	1.675
AIRFOIL Y_0 199	0010 MOD	WEDGE
SWEEP (LEADING EDGE)	45°	45°
(WING GLOVE)	81°	
M.A.C.	474.81 IN.	199.81 IN.
DIHEDRAL (TRAILING EDGE)	3.5°	

CONTROL SURFACE AREA AND MAX DEFLECTION

AREA		MAX DEFLECTION
ELEVON (ONE SIDE)	210 FT^2	35° TO +20°
RUDDER	100.15 FT^2	+22.8°
SPEED BRAKE	100.15 FT^2	0° TO 87.2°
BODY FLAP	135.0 FT^2	11.7° TO +22.55°

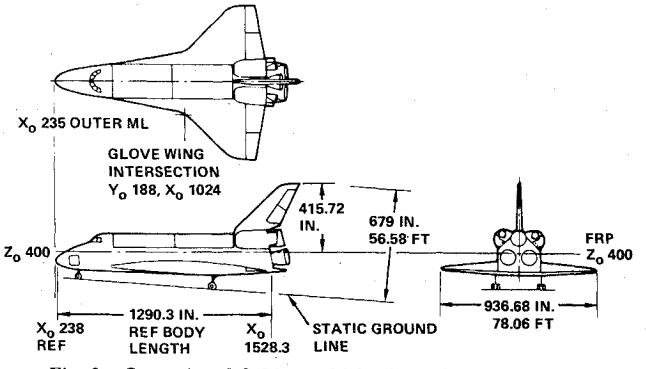

Fig. 9 Operational Orbiter vehicle dimensions (vehicle 5).

to apply drag modulation for the subsonic flight phase, approach, and landing. The section profile is a 5-deg half-angle, 60 to 40% double-wedge airfoil. Aerodynamic control surfaces consist of full-span elevons for pitch and roll control, a conventional rudder for yaw control, and speed brakes formed by deploying symmetrical halves of the rudder through equal angles. A body flap was also employed to aid hypersonic pitch trim and to shield the SSME rocket nozzles. Additional development studies were performed to refine and optimize Orbiter geometry. These studies included optimizing wing twist and camber, wing-body blending, forebody camber, and corner radius.

After the wing geometry required for landing speed constrained to vehicle weight was established, effects of glove (leading delta) size, wing twist, and camber were investigated. The glove was sized to provide ample stall margin, $C_{L_{max}}$, and to provide the design static margin at the aft center of gravity. Increasing glove size increased $C_{L_{max}}$ and relocated the aerodynamic center forward, yielding a higher trim C_L. Further refinements, such as glove leading-edge radius, wing glove fillet, planform geometry, and optimal wing camber resulted in a 20% increase in trimmed lift (Fig. 8).

The requirements for a drogue parachute were evaluated based on programmatic cost and weight decisions. The drogue parachute was eliminated as a result of these studies. In addition, the docking hatch and airlock were deleted which resulted in shortening the Orbiter by several feet. Based on weight constraints, the OMS pods forebody fairing was shortened. The payload manipulator arm housing (on top of the fuselage from the canopy to the vertical) was placed inside the payload bay doors.

Later programmatic and technical refinements have produced the current Orbiter configuration (CDR vehicle, Fig. 9) with a down payload of 32,000 lb, design landing velocity of 171 knots at an angle of attack of 15 deg, and a design center of gravity range of 2.5% body length with −2% static margin at the aft center of gravity limit (67.5% body length).

Aerodynamic Characteristics of the Baseline Orbiter

Current estimates of Orbiter flight characteristics are based on a continuing, extensive wind tunnel test program. The extreme range of flight conditions inherent in Shuttle missions requires aerodynamic data over a Mach number range from low speeds with incompressible flow conditions to hypersonic orbital entry conditions where real-gas effects and viscous interaction phenomena may be significant. Large angle-of-attack and control deflection ranges introduce various problems of flow separation prediction. A relatively large design center of gravity range and multiple uses and combinations of the vehicle's control surfaces further increase the magnitude and complexity of the task of defining the Orbiter's aerodynamics.

Entry Flight Mode

The baseline entry trajectory and flight profile illustrating flight control modes are shown in Fig. 2. There are two different control modes—spacecraft and aircraft. Pitch control during the spacecraft mode is obtained from reaction control system (RCS) units until the dynamic pressure reaches 2 psf, at which time elevons are actuated. RCS and elevons are employed for pitch control until the dynamic pressure reaches 20 psf, when the pitch RCS units are deactivated and elevons are employed for the remainder of entry. Roll control is furnished by RCS until a dynamic pressure of 2 psf is attained, at which time ailerons are activated. RCS is used to assist in roll control until dynamic pressure reaches 10 psf, when they are deactivated. RCS is used for yaw control until a velocity of approximately 1500 fps is attained and the transition to the aircraft mode is completed. The rudder is actuated at a velocity of 4000 fps and provides rudder control until touchdown. The speed brake is programmed to assist pitch trim and augment lateral stability during entry. On approach and landing, speed brake setting is modulated for velocity control.

Static longitudinal trim and stability requirements are satisfied along design entry trajectories as illustrated in Fig.

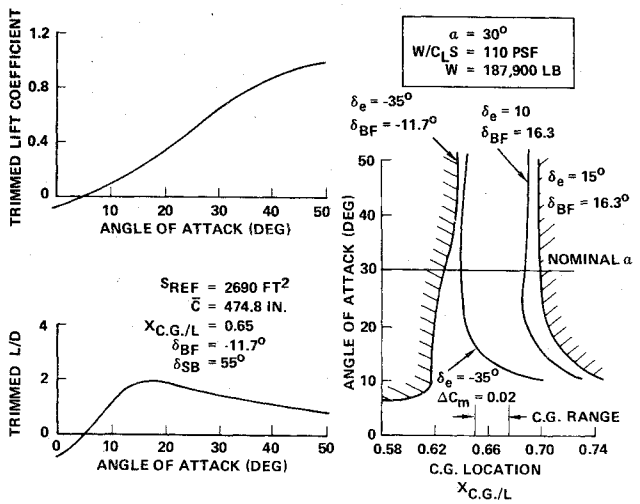

Fig. 11 Orbiter hypersonic longitudinal aerodynamic characteristics.

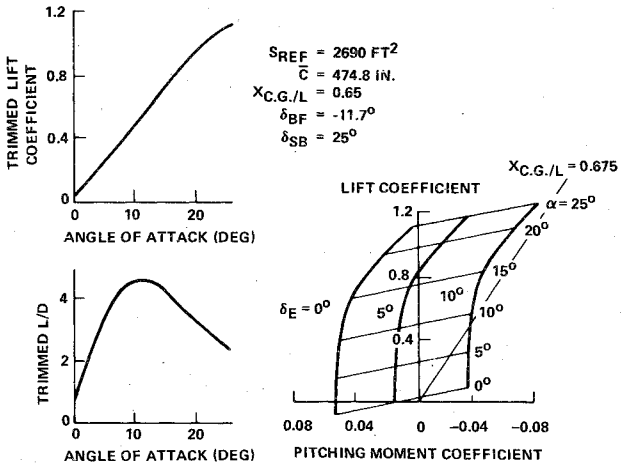

Fig. 13 Orbiter longitudinal aerodynamic characteristics (low speed).

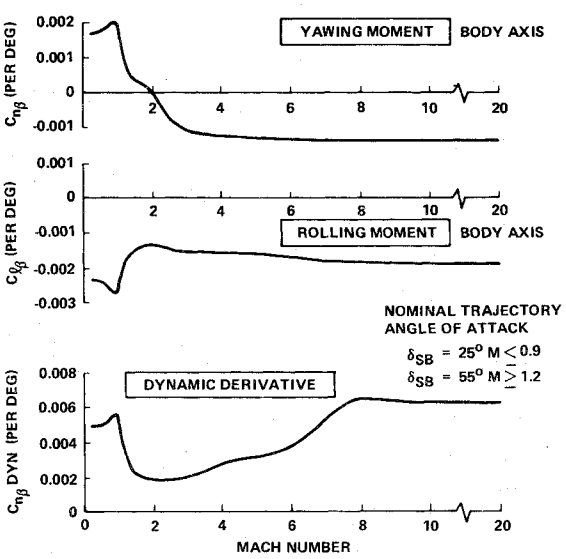

Fig. 12 Lateral-directional characteristics.

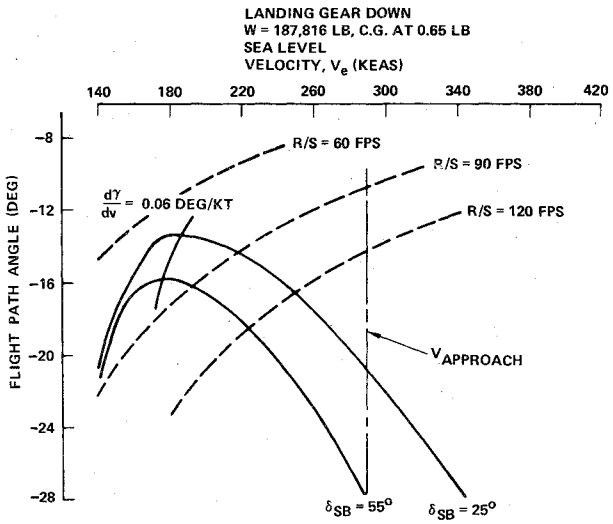

Fig. 14 Orbiter landing performance characteristics.

10. The desired pitch trim capability has been achieved by taking advantage of the pitch effectiveness of the body flap and speed brake, used in conjunction with the elevons. It should also be noted that the static control limit boundaries shown include incremental pitching moment reserves for maneuvering and aerodynamic data uncertainties.

High-Speed Characteristics

Hypersonic longitudinal flight characteristics without viscous interaction effects are summarized in Fig. 11. Values of hypersonic lift coefficient and lift-to-drag ratio have been maintained at levels consistent with aeroheating constraints and trajectory requirements. The pitch trim range is sufficiently wide and well centered with respect to the design center of gravity range.

Lateral-directional characteristics of the Shuttle Orbiter are presented in Fig. 12 for angles of attack along a nominal entry trajectory. The directional stability derivative (C_{n_β}) is positive, indicating static stability in yaw, at Mach numbers below 2; above Mach 2, C_{n_β} is negative. However, the dihedral stability derivative (C_{l_β}) is sufficiently negative (stable in roll) that the dynamic derivative $(C_{n_\beta})_{\text{dyn}}$ is positive along the entire trajectory. Positive $(C_{n_\beta})_{\text{dyn}}$ is a necessary condition for Dutch roll stability.

Viscous interaction effects are encountered for values of the viscous parameter $V'_\infty = M_\infty \sqrt{c'_\infty}/\sqrt{R_{e_\infty}'}$ from 0.007 to 0.1, the latter value corresponding to an altitude range from 200,000 ft to 300,000 ft. Viscous interaction reduces lift-to-drag ratio and the forward center of gravity control limit.[2] During RCS usage, the RCS exhaust interact with the Orbiter flowfield to influence RCS effectiveness. Consequently, wind tunnel simulation of RCS operation has been performed and correction factors developed to account for this interaction.[2]

Low-Speed Characteristics

Low-speed longitudinal aerodynamics are illustrated in Fig. 13 for the forward center of gravity. The trimmed lift is adequate to keep the touchdown velocity below the nominal design maximum of 171 knots for a design touchdown angle of attack of 15 deg, and the subsonic maximum lift-to-drag ratio is greater than the minimum contract end item (CEI) specification of 4.4. For low-speed conditions, the Orbiter is adequately trimmed with positive elevon deflections as indicated in the pitching moment/lift diagram (Fig. 13).

Ranges of approach speed and flight path angles are indicated in Fig. 14. It is noted that the flight path stability parameters $d\gamma/dv$ are negative (stable) over most of the approach ($d\gamma/dv < 0.06$ deg/knot is a MIL Spec requirement). The effects of speedbrake deflection for drag modulation are also illustrated. Touchdown speeds can vary over a wide range (extremes of 134 knots to 221 knots) depending primarily on Orbiter payload weight and required angle of attack with off-nominal values allowing for winds and variations in approach conditions.[3] The Orbiter can land on a 10,000-ft runway as required.[3]

Conclusion

The Space Shuttle Orbiter configuration has been finalized and manufacture of the initial vehicle, to be employed in approach and landing test, has been completed. Flight tests were conducted in 1977 for the approach and landing test flight phase. The entry Orbiter configuration is in final manufacture and assembly with first manned orbital flight scheduled for early 1979. A mature aerodynamic data base has been developed and no major problems have been uncovered.

Acknowledgments

The Orbiter aerodynamic activities described herein were accomplished by a team of Rockwell International and NASA personnel. Significant contributions were made by the following: W.E. Bornemann of Rockwell and B. Redd and J.C. Young of NASA/Johnson Spacecraft Center.

References

[1]Hoak, D.E. and Finck, R.D., "USAF Stability and Control DATCOM," Wright Patterson Air Force Base, Ohio, AFFDL, Jan. 1974.

[2]*Aerodynamic Design Data Book, Volume I, Orbiter Vehicle,* Rockwell International, Space Division, Report No. SD 72-SH-0060-1J, Dec. 1975.

[3]Surber, T.E. and Olsen, D.C., "Space Shuttle Orbiter Aerodynamic Development," AIAA Paper 74-991, Los Angeles, Calif., Aug. 1974.